

# Experimental study of fire tornado

A.M. Grishin,<sup>2</sup> V.V. Reino,<sup>1</sup> V.M. Sazanovich,<sup>1</sup>  
R.Sh. Tsyvk,<sup>1</sup> and M.V. Sherstobitov<sup>1</sup>

<sup>1</sup>*Institute of Atmospheric Optics,  
Siberian Branch of the Russian Academy of Sciences, Tomsk*  
<sup>2</sup>*Tomsk State University*

Received August 29, 2007

Results of fire tornado study under model conditions are presented. The tornado was formed through airflow twisting by blades, rotary under a stationary tank filled with a burning substance (spirit). The dependence of the heat flow, rate of burning, frequency of spectral maxima of the image centroid jitters, and tornado-transmitted laser radiation intensity fluctuations on the blade revolution rate is found.

## Introduction

In recent years, the coherent structures, including, in particular, various tornados and swirling flows, are of increasing interest. The results of theoretical and experimental investigations of physical characteristics of whirlwinds and tornados, the conditions for their formation and stability were considered earlier.<sup>1–8</sup> The medium in such flows is complicated and random, where spatiotemporal fields of temperature, speed, and refraction index continuously fluctuate.

The conditions for tornado-like vortex formation over a rotating heated disk in dead air were experimentally studied in Ref. 1. The vortex was visualized by means of rosin evaporation from the disk surface. It has been shown that a tornado-like heat vortex arises at a disk rotation speed of about  $(2.3 \pm 1.5)$  rev./s. Speed increase or decrease results in burning breakdown in the vortex mode and transfer to swirling turbulent flow. Such type of tornado is conventionally called “heat.”

Some physical characteristics of a fire tornado, excited via rotating a tank filled with a burning substance, were considered in Refs. 8, 9, and 12, where a stable tornado was also formed in limited rotation speed ranges  $[(1 \pm 0.2),^8 3.8 \pm (0.2 \div 0.4)$  rev./s].<sup>12</sup>

A mathematical model for forecasting the dynamics of fire formation in open fire conditions is known; it has been developed based on numerical solution of the generalized set of equations for unstable two-dimensional turbulent motion of viscous compressible gas with accounting for burning.<sup>7</sup> Features of fire tornados have been determined. The principal conclusions are the following: the tornado has the form of vertical cylinder 2–3 times higher than that at diffusion burning, the temperature is almost invariable with height, and axis pressure is less than in the ambient air.

Some first results on fluctuations of parameters of a laser beam, propagating through a convective column and swirling flame jet (which is the model of fire tornado), are given in Refs. 10 and 11.

Note, that the study of physical parameters of the burning process in tornado conditions and its optical parameters is in the early stage. Tornado sizes, fuel-burning rates, components of the motion speed in the flow, turbulent conditions, and some other burning parameters as functions of tornado rotation speed and way of its swirling need to be precised.

In this work, the rotation-speed dependence of the following tornado parameters is studied: the heat flow; burning rate; frequencies of maxima of spectral functions of image centroid jitters, and intensity of the tornado-passed laser radiation. The tornado, in contrast to the modeled<sup>12</sup> vortex, was formed by twisting the airflow by blades rotary under a stationary tank filled with a burning substance. Such model technique allows a stable tornado formation in a wide range of revolution rates. Note that measurement of flow motion speed, especially of its radial component, is a nontrivial problem, which can be solved by optical methods.

## Measurement equipment and technique

The experimental setup is schematically shown in Fig. 1.

A fixed tank of 142 mm in diameter and 17 mm in height is filled with the burning matter (20–30 ml of spirit). An adjustable-speed motor with axel-mounted blades is placed under the tank. The blades produce an ascending swirling airflow around the tank. The motor speed was measured with a frequency meter from optical sensor pulses. The heat flow was measured with a heat flow sensors, located at 0.32, 0.5, and 0.8 m from the fire. The data were registered in the measuring block with following input into a computer. The brightness temperature distribution in the tornado was measured with an Inframetric thermal imaging system within the 3–12  $\mu$ m wave range. Scale coefficients were calculated by the measured distances between images of three lamps, spaced horizontally and vertically by 50 cm.

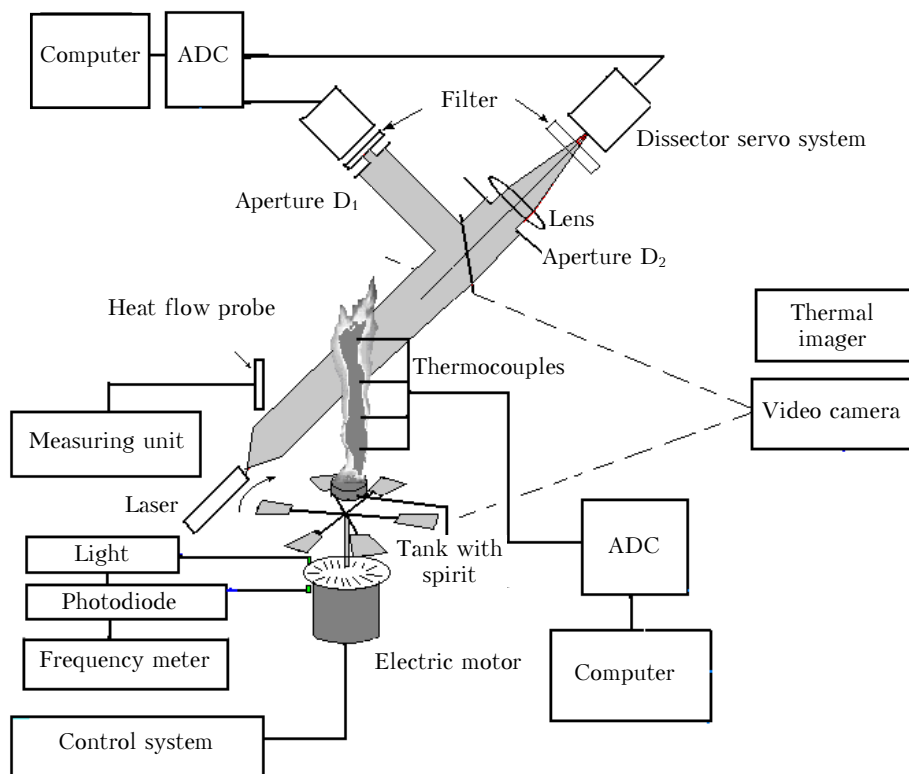


Fig. 1. Block-diagram of the experimental setup.

The tornado height and diameter, height temperature distribution along the axis, maximal and average temperatures were determined from the images. Burning time from the firing moment to complete fuel combustion was recorded.

A collimated laser beam of 2 cm in diameter (the source was a laser with  $\lambda = 0.532 \mu\text{m}$ ) passed through the fire at a height of 100 m above the level of burning liquid and was divided into two channels with a beam splitting cube. A photomultiplier with the aperture  $D_1 = 0.1 \text{ mm}$  was mounted in the first channel. A lens with the aperture  $D_2 = 10 \text{ mm}$  and a dissector servo system in the lens focus was mounted in the second channel for measuring horizontal and vertical jitters of the radiation source image centroid.

The measurements were carried out in the diffusion-burning mode (without swirling) and with flow swirl at revolution rates from 2 to 16 rev./s.

## Measurement results

The examples of tornado image (256×256 pixels) obtained with the thermal imaging system are shown in Fig. 2 for different motor speeds. The temperature scale and its maximum are shown to the left of each image.

The images were processed with a program going along with the thermal imaging system.

As is seen in Fig. 2 at a motor speed of 2 rev./s, the fire shape is close to cylindrical up to 0.5–0.75 of

the tornado height, then the fire rises and stretches, acquiring the form of a narrow cord. A similar tornado shape is recorded with the video camera in the visible range. Note, that the tornado is formed in the narrow rotation speed range  $[3.8 \pm (0.2 \div 0.4) \text{ rev./s}]$ , the upper part of tornado is unstable with noticeable flameouts in different directions.<sup>12</sup>

Figure 2 shows brightness temperature height distribution along the axis, the vertical and horizontal lines show the tornado height and measurement point in a horizontal section. These distributions are exemplified in Fig. 3.

Oscillating character of brightness temperature distribution in height follows from data analysis. The amplitude of these oscillations is 6–14 cm and connected with the presence of cords in the tornado structure well prominent in the visible range.<sup>11,12</sup> The average temperature slowly decreases to 0.5–0.75 of tornado height and then drops. Such conclusion agrees with the calculation results.<sup>7</sup> The brightness temperature distribution in a horizontal section in the tornado conditions is properly described by the equation  $T(x) = T_m \exp[-((x - x_m)/R)^2]$ , where  $T_m$  and  $x_m$  are the maximal temperature and its coordinate;  $R$  is the distribution half-width at  $1/e$  level.<sup>12</sup> An example of such approximation is shown in Fig. 3b for one of the distributions.

When processing the thermal vision images, the average integral radiant emissivity of fire  $\varepsilon = 0.5$  was introduced for temperature calculations.<sup>13</sup> The thermocouple-measured temperature was  $T_1 \sim 1000 \text{ K}$ .

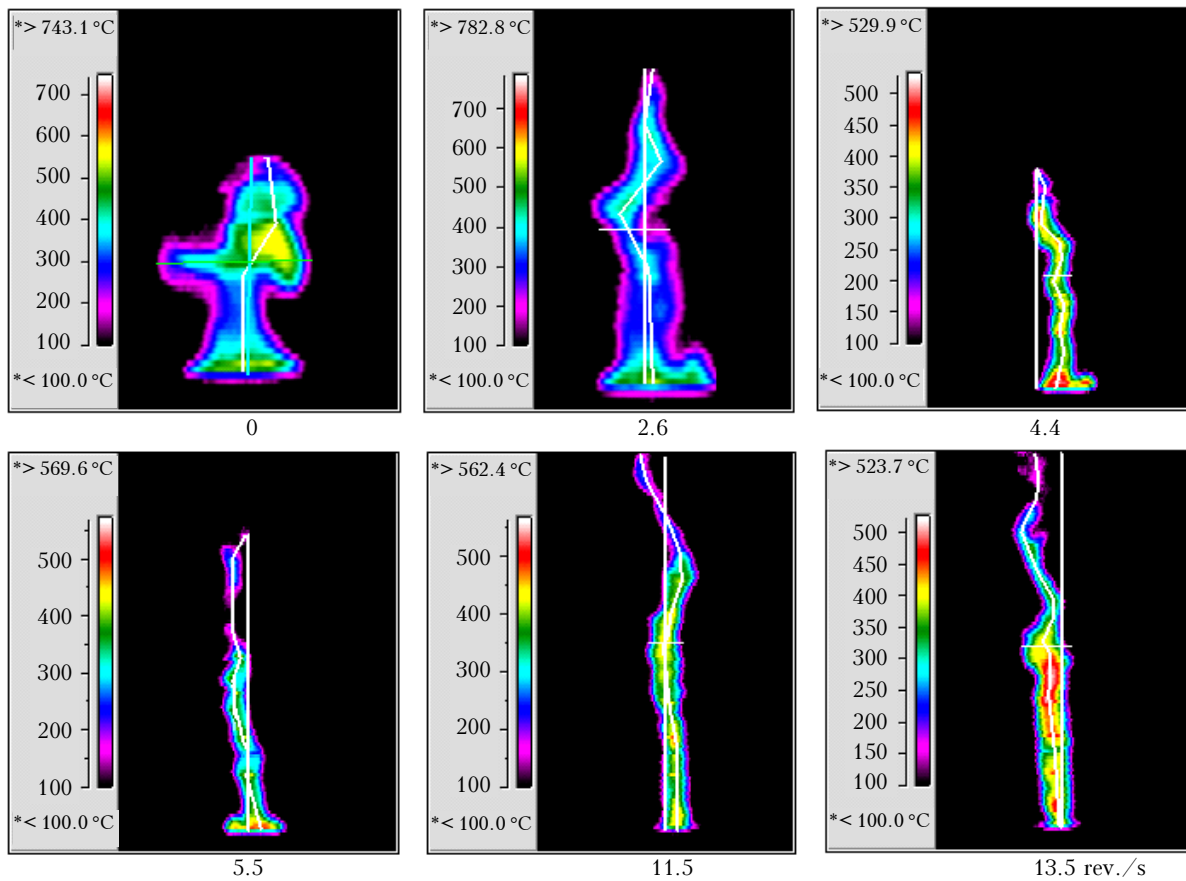


Fig. 2. Thermal vision tornado images at different motor speeds.

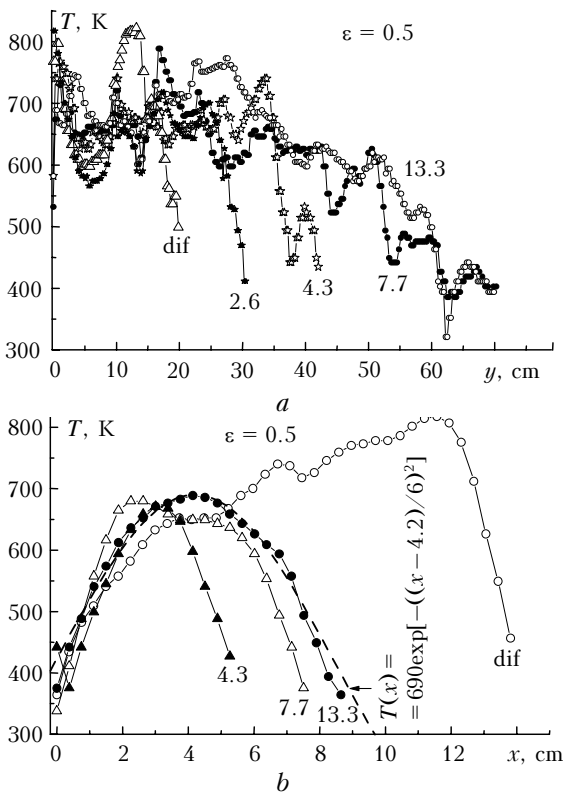


Fig. 3. Brightness temperature distributions over the vertical tornado axis (a) and in a horizontal section (b).

Another radiant emissivity  $\epsilon_1$  should be used for agreement between the temperatures, measured with a thermal imaging system within the 5–12  $\mu\text{m}$  range and with thermocouples when spirit burning. This parameter can be calculated from the relation  $\epsilon T^4 = \epsilon_1 T_1^4$ :  $\epsilon = 0.5$ ,  $T = 750\div 850$  K, and  $T_1 = 1000$  K,  $\epsilon_1 \approx 0.16\div 0.26$ . The decrease of the radiant emissivity relates to the fact that the radiant emissivity for a weakly smoking fire is determined by the concentration of basic emitting combustion products, i.e., carbon dioxide and water vapors.<sup>14</sup>

The tornado height and diameter were determined by the temperature close to background by the least square method. The results are shown in Fig. 4. The parameters evidently rise as the rotation speed increased.

The time variations of heat-flow rate, measured with the heat flow sensor, are shown in Fig. 5a for different rotation speeds. The sensor time constant is about 30 s.

The measurements were performed at different distances  $L$  from the tornado. To compare the measurement results, it was supposed that the tornado is a rectangular emitter with the height  $H$  and width  $d$ , emitting the total effective flow  $P_0$ . Each elementary unit of the tornado is a source of spherical waves. Then the calculated heat-flow rate (irradiance)  $P_m$  at a sensor [Ref. 15] with accounting for the distance between the sensor and each tornado point is

$$P_m = P_0 \arctan(H/2L)/HL. \quad (1)$$

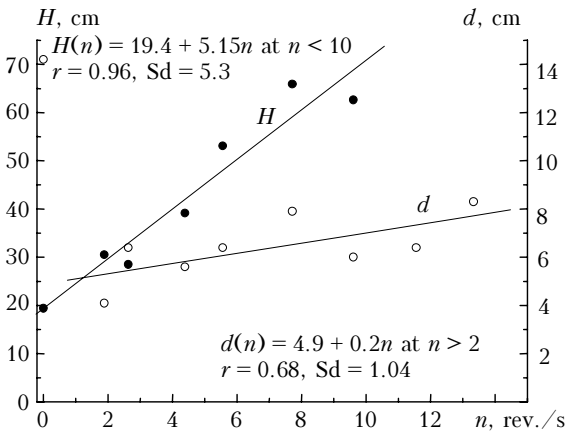


**Fig. 4.** The tornado height  $H$  and its diameter  $d$  as functions of motor speed  $n$  ( $r$  is the correlation factor and  $Sd$  is the rms variation).

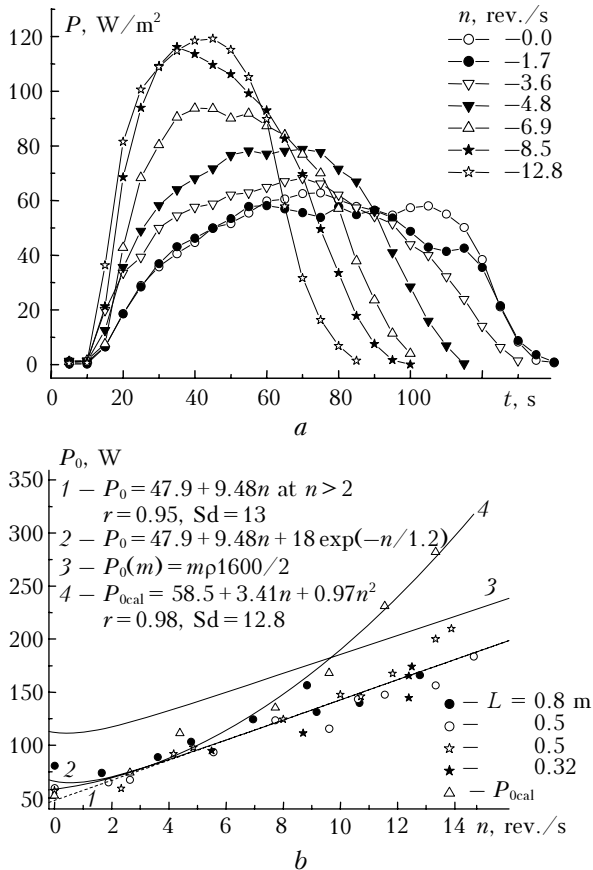


**Fig. 5.** Heat flow rate  $P$  as a function of time  $t$  (a) and motor speed  $n$  (b),  $P_0$  is the measured tornado effective flow,  $P_{ocal}$  is the assessed tornado heat flow,  $P_0(m)$  is the heat flow calculated from the fuel-burning rate (considered below).

Knowing the measured  $P_m$  values ( $W/m^2$ ), defined as maximal values of the heat flow sensor (Fig. 5, a), the total effective tornado heat flow  $P_0$  (W) can be calculated within the wavelength range of the thermal imaging system:

$$P_0 = P_m H L / \arctan(H/2L). \quad (2)$$

In this case,  $P_0$  is independent of the distance. Results of the analysis are given in Fig. 5, b, where curve 1 was calculated by the least-square-method for  $n > 2$  and curve 2 was obtained by the fitting method with accounting for the straight-line equation, sufficiently accurate describing  $P_0$  within the whole motor speed range.

The total effective heat flow of tornado was assessed with the following processing technique.

The heat flow from a surface of the area  $S$  is<sup>15</sup>

$$P_{ocal} = \varepsilon_1 \sigma T^4 S, \quad (3)$$

where  $\sigma = 5.67 \cdot 10^{-8} W/(m^2 \cdot K^4)$ ;  $\varepsilon_1 = 0.25$ . Here the average value  $T^4 = \langle T(y)^4 \rangle$ , calculated over the measured height distributions of temperature (see Fig. 3), is taken as the temperature value. The temperature was converted from Celsius to Kelvin degrees with accounting for the real radiant emittivity  $\varepsilon_1 = 0.25$ .

The fire area was calculated using the experimental regression equations for height and diameter (see Fig. 4):

$$S(n) = H d_c = H d / 1.4 = 10^{-4} (19.4 + 5.15n) (4.9 + 0.2n) / 1.4 m^2. \quad (4)$$

It was shown in Ref. 12, that the standard average distribution of brightness temperature in a tornado horizontal section is sufficiently well described by the gaussoid  $T(x, y) = T(y) \exp[-(x/R)^2]$  with the effective half-width  $R$ , determined at the  $1/e$  level. When processing images, the diameter  $d$  was determined at the background level  $T(x, y)/[T(y)] = 1/(2e)$ . Therefore, the coefficient, correlating the effective  $d_c = 2R$  and measured  $d_m = d/2^{0.5}$  diameters was introduced in  $S(n)$  calculation. The temperature height distribution  $T(y)$  was taken from measurements.

The results of  $P_{ocal}$  assessment are shown in Fig. 5b and satisfactorily agree with the experimental data in view of the fact that the tornado is a cone (but not a cylinder) at heights of  $(0.5-0.75)H$ . Curve 4 here was calculated by the least square method.

Figure 6 shows the motor-speed dependences of the fuel-burning rate  $m$  and frequencies of maximum of the spectral function  $f_m$  of the intensity fluctuations, and jitters of the image centroid of a fire-passed laser beam.

The burning rate has been calculated as  $m = M/t$ , where  $t$  is the burning time and  $M$  is the initial fuel volume. The frequency of the spectral maximum of image centroid jitters of a fire-passed laser beam has been determined by the calculated spectral functions  $U(f) = fW(f)$ , where  $W(f)$  is the fluctuations spectral density similar to the obtained earlier.<sup>11</sup> The curves were calculated by the technique, similar to those, used in the total flow processing (see above).

As is seen from Figs. 5b and 6, the basic tornado parameters (height, diameter, effective heat flow, fuel-burning rate) and image jitters of the laser beam, propagating through the tornado, grow linearly at the motor speed  $n > 2$  rev./s.

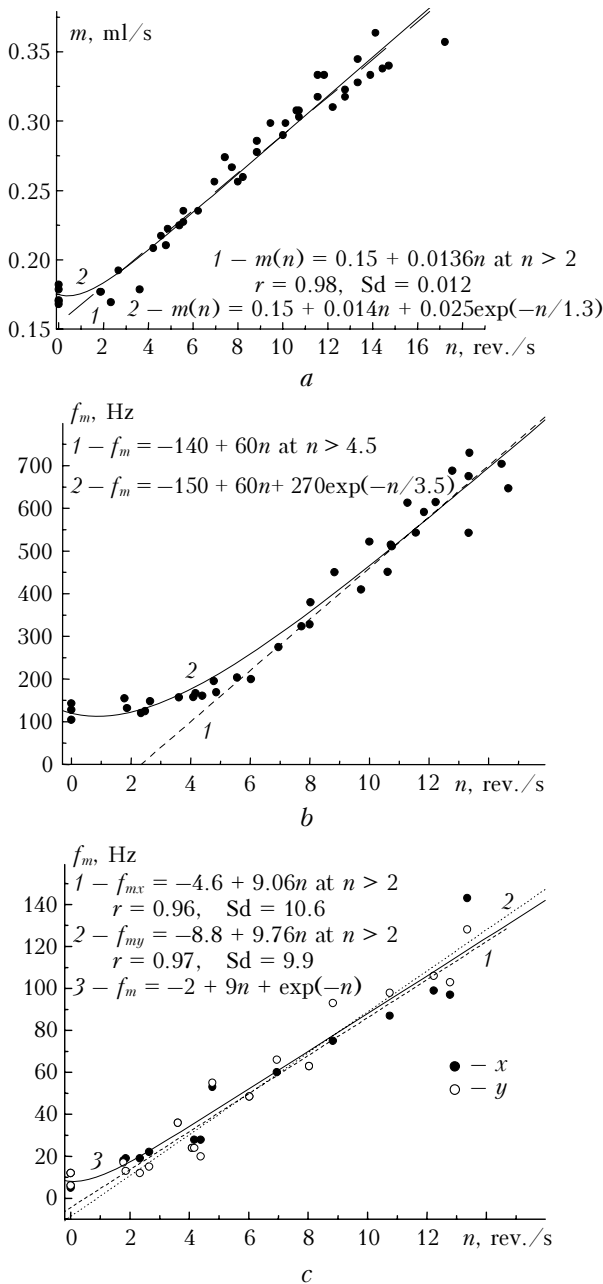


**Fig. 6.** The fuel-burning rate  $m$  (a) and frequencies of the spectral maximum of intensity fluctuations (b) and laser beam image centroid jitters (c) as functions of motor speed ( $x$  is the horizontal and  $y$  is vertical coordinates).

The frequency of spectral maximum intensity fluctuations is observed at  $n > 5$  rev./s, because the internal structure of tornado (cords), mainly influencing the intensity fluctuations, is formed in steady-state conditions at  $n > 5$ .<sup>11</sup> All the above-listed parameters  $G(n)$  with accounting for transition section at  $n \geq 0$  are well described by the equation

$$G(n) = a + bn + c \exp(-n/k), \quad (5)$$

where  $a$ ,  $b$ ,  $c$ , and  $k$  are constants, depending on the measured parameter.

If the fuel-burning rate is known, the tornado-emitted heat flow can be calculated. It is known, that the heat  $P_c = 1600$  W/g is released when burning 1 g of spirit. Hence, the heat flow, released toward the heat flow sensor, is

$$P_0(m) = m\rho P_c/2 = [0.15 + 0.014n + 0.025\exp(-n/1.3)] 0.8 \cdot 1600/2 \text{ W/s}, \quad (6)$$

where  $m$  is the fuel-burning rate, ml/s (Fig. 6a);  $\rho = 0.8$  g/ml is the spirit density.

The calculation results are shown in Fig. 5. As it is evident from Fig. 5b, the  $P_0(m)$  values exceed the  $P_{0\text{raz}}$  at a close motor-speed dependence. This is connected with the fact that a part of heat whirls away into the hot convective column above the fire. In this case, the convective column emits insignificantly.

### Conclusions

The main results of the study of physical and optical tornado parameters when swirling fire by an external airflow (motor with blades) and a fixed tank with fuel, are the following.

1. Formation of the stable tornado begins at the revolution rate  $n > 2$  rev./s and keeps almost up to complete fuel combustion at a revolution rate up to 18 rev./s (experimental results). When swirling by rotating a tank with fuel, a stable tornado is formed at a limited revolution rate ( $\sim 3.8$  rev./s) and sometimes breaks during firing.

2. The maximal thermocouple-measured temperatures take place about  $\sim 800$ – $1100$  K, while measured with a thermal imager at  $\epsilon = 0.5$  –  $700$ – $800$  K. To make the temperatures closer, the radiant emissivity  $\epsilon \sim 0.16$ – $0.26$  should be used within the  $3$ – $12$   $\mu\text{m}$  range, since weakly smoking fire is formed when spirit burning. It is known, that the smokiness lowering results in  $\epsilon$  decrease.<sup>14</sup>

3. The tornado is close to a cylinder up to the height  $(0.5$ – $0.75)H$  and its temperature slowly decreases, which supposes a uniform fuel burning rate here. The upper part of tornado higher than  $(0.5$ – $0.75)H$  stretches to a cone and flickers (similar to candle light), and its temperature drops.

4. The tornado height, diameter, and effective heat flow, as well as the fuel-burning rate grow linearly with the motor speed (at  $n > 2$  rev./s). These parameters (with accounting for transition section of tornado) are adequately described by the equation  $a + bn + c \exp(-n/k)$  for all  $n$  (see Figs. 5b and 6).

5. The frequency of spectral maximum of intensity fluctuations of the laser beam, passing through the tornado, grows linearly at the motor speed  $n > 5$  rev./s. Such behavior of the image centroid jitters is observed at  $n > 2$  rev./s. This difference is explained by the fact that the intensity fluctuations are mainly affected by the internal structure of tornado (medium fluctuations of small scales), formed in steady-state conditions at  $n > 5$ . The image centroid jitters are mainly influenced by the scales, comparable or larger than the sizes of the receiving lens (1 cm in our experiments).<sup>16</sup>

6. Linear relationship between the fluctuation maximal frequency of laser beam parameters and motor speed is promising for developing optical (remote) methods for measuring the components of flow motion speed immediately in the tornado.

### References

1. B.M. Bubnov, *Izv. Ros. Akad. Nauk. Fiz. Atmos. Okeana* **33**, No. 4, 434–442 (1997).
2. A.M. Grishin, A.N. Golovanov, and Ya.V. Sukov, *Dokl. Ros. Akad. Nauk* **395**, No. 2, 196–198 (2004).
3. A.M. Grishin, *Modeling and Catastrophe Forecasting* (Publ. House of TSU, Tomsk, 2003), 522 pp.
4. S.V. Alekseenko, P.A. Kuibin, and V.L. Okulov, *Introduction into Concentrated Vortexes Theory* (Publ. House of the Inst. of Thermal Physics SB RAS, Novosibirsk, 2003), 504 pp.
5. L. Bengtsson and J. Lighthill, eds., *Intense Atmospheric Vortexes* (Mir, Moscow, 1985), 368 pp.
6. G.F. Carrier, F.E. Fendell, and P.S. Feldman, *Teploperedacha* **107**, No. 1, 6–25 (1985).
7. Yu.A. Gostintsev and A.M. Ryzhov, *Izv. Ros. Akad. Nauk. Mekh. Zhidkosti i Gaza*, No. 6, 52–61 (1994).
8. A.M. Grishin, A.N. Golovanov, A.A. Strokotov, and R.Sh. Tsvyk, *Dokl. Ros. Akad. Nauk* **400**, No. 5, 618–620 (2005).
9. A.M. Grishin, A.A. Dolgov, V.V. Reino, R.Sh. Tsvyk, and M.V. Sherstobitov, in: *Proc. of Intern. Conf. on Forest and Steppe Fires: Origination, Spread, Extinguishing, and Ecological Consequences* (Irkutsk, 2001), pp. 63–66.
10. V.M. Sazanovich and R.Sh. Tsvyk, *Atmos. Oceanic Opt.* **15**, No. 4, 336–343 (2002).
11. A.M. Grishin, V.M. Sazanovich, A.A. Strokotov, and R.Sh. Tsvyk, *Atmos. Oceanic Opt.* **19**, No. 12, 935–939 (2006).
12. A.M. Grishin, A.N. Golovanov, V.V. Reino, V.M. Sazanovich, A.A. Strokotov, R.Sh. Tsvyk, and M.V. Sherstobitov, *Atmos. Oceanic Opt.* **20**, No. 3, 215–219 (2007).
13. L.A. Mirzoeva, G.B. Kameshkov, E.L. Lustberg, G.A. Makovtsev, and G.V. Zakharenkov, *Opt. Zh.*, No. 8, 17–21 (1992).
14. L.Z. Kriksunov, *Handbook on IR Technique Principles* (Sov. Radio, Moscow, 1976), 400 pp.
15. B.A. Grigor'ev, *Radiation Pulse Heating*. P. 1 (Nauka, Moscow, 1974), 320 pp.
16. V.E. Zuev, V.A. Banakh, and V.V. Pokasov, *Optics of Turbulent Atmosphere* (Gidrometeoizdat, Leningrad, 1988), 272 pp.